

On the Non-Ideal Behaviour of Polarised Liquid-Liquid Interfaces

Marco F. Suárez-Herrera^{*,a,b} and Micheál D. Scanlon^{*,a,c}

^a The Bernal Institute, University of Limerick (UL), Limerick V94 T9PX, Ireland.

^b Departamento De Química, Facultad De Ciencias, Universidad Nacional De Colombia, Cra 30 # 45-03, Edificio 451, Bogotá, Colombia.

^c Department of Chemical Sciences, School of Natural Sciences, University of Limerick (UL), Limerick V94 T9PX, Ireland.

*E-mail: mfsuarezh@unal.edu.co

*E-mail: micheal.scanlon@ul.ie

Abstract

Interpretation of electrochemical data generated at the interface between two immiscible electrolyte solutions (ITIES), and realisation of the ITIES for technological applications, requires comprehensive knowledge of the origin of the observed currents (*i.e.*, capacitive, ion or electron transfer currents) and the factors influencing the electrical double layer. Upon formation, the ITIES is away from equilibrium and therefore is a close approximation, but not a perfect realisation, of an ideally polarisable interface. Nevertheless, the formalism of equilibrium thermodynamics, *e.g.*, the Nernst equation, are universally applied to interpret electrochemical processes at the ITIES. In this study, electrochemical impedance spectroscopy (EIS), cyclic and AC voltammetry were applied to probe electrochemical processes at an ITIES formed between aqueous and α,α,α -trifluorotoluene electrolyte solutions. A significant contribution from faradaic currents is observed across the whole polarisable potential window and the electrolyte solution is not an ideal resistor (especially at high electric field frequencies). The electrical double-layer at the interface is influenced by the nature of the ions adsorbed. Small inorganic ions, such as sulfate anions and aluminium cations, are shown to adsorb at the interface, with methanesulfonic acid adsorbing

strongly. The nature of ions adsorbed at the interface shifts the potential of zero charge (PZC) at the ITIES, which we propose in turn influences the kinetics of ion transfer.

Keywords

Interface between two immiscible electrolyte solutions; liquid-liquid interface; electrical double layer; electro-adsorption; potential of zero charge

1. Introduction

The interface between two immiscible electrolytic solutions (ITIES) provides a versatile platform for charge transfer reactions. Electrochemical reactions at these polarised liquid-liquid (L-L) interfaces can take the form of ion transfer from one phase to the other, heterogeneous or photo-induced electron transfer between species in the opposite phases, and adsorption-based charge transfer events[1,2]. The versatility of charge transfer events possible at the ITIES is now being matched by the variety of applications being reported, which spans from sensor development [3] to redox electrocatalysis [4,5], photo-energy conversion[6,7], and nanomaterial self-assembly [8–10]. The current understanding of electrochemical phenomena occurring at the ITIES has been well documented in many reviews and books[11,12]. The ITIES is approximately 1 nm in width, with two back-to-back diffuse double layers and a Helmholtz layer of compact ions between them [13,14]. Typical organic solvents used to form an ITIES are α,α,α -trifluorotoluene (TFT) and 1,2-dichloroethane (DCE). The properties of this electrical double layer affect all processes that take place at the L-L interface, *e.g.*, the kinetics of ion transfer, heterogeneous electron transfer, and electrocatalytic reactions.

Electrochemical techniques such as cyclic voltammetry (CV), alternating current (AC) voltammetry, electrochemical impedance spectroscopy (EIS) and chronoamperometry are widely used to study charge transfer events at the ITIES using a specialised 4-electrode electrochemical cell. Herein, we discuss the interpretation of data from EIS, a task that is often difficult due to the perceived presence of artefacts in such spectra, especially at high frequencies.[15] We provide an understanding of EIS spectra at

the ITIES across a broad range of frequencies, from 500 kHz to 0.1 Hz. Furthermore, we discuss the mechanism by which the potential drop at the L-L interface changes when the potential difference between the two counter electrodes is changed.

When two immiscible electrolyte solutions such as aqueous and organic electrolyte solutions are brought into contact, the system is away from thermodynamic equilibrium. Without an external perturbation (*i.e.*, at open circuit potential, OCP) the system takes hours to reach a constant interfacial energy that matches the OCP. In this regard, Mareček and co-workers recently reported a new experimental configuration to record the interfacial potential from the first contact of the two electrolytes [16,17]. Recording of the OCP began when both phases were separated by an air bubble inside the tip of a capillary. The bubble was then ejected by a syringe connected to the capillary, the solutions came into contact, and the transient OCP was measured until equilibrium was reached. Nevertheless, the analysis of data generated at the ITIES typically involves the formalism of equilibrium thermodynamics, *e.g.*, the Nernst equation. However, during cyclic polarisation, the L-L interface is clearly away from thermodynamic equilibrium and permeable to ions to some extent at open circuit potentials and across the whole potential window. Herein, we probe the contribution from capacitive and faradaic processes to the currents measured across the whole potential window when a L-L interface is polarised. In other words, we explore if the currents in the middle of the potential window are primarily capacitive?

Differential capacitance measurements at the ITIES have been reported to depend on the nature of, and interactions between, ions present in both phases [18,19]. However, the microscopic origin of this differential capacitance is still a matter of debate [20,21]. For example, it is not clear if ion pairs form at the interface [22], what is the effect of electrocapillary waves during alternating current (AC) experiments [23], and if small inorganic ions, such as alkaline or aluminium cations, sulfates, *etc.*, can adsorb at the interface. To obtain a deeper understanding of the structure of the electrical double layer at the L-L interface, more in-depth studies of interfacial ion adsorption are key. Herein, we present the adsorption of simple ions (such as protons, methanesulfonate or sulfate anions, and aluminium cations) at the ITIES, and hope that this work will be beneficial to expand on previous studies in this regard [18–28].

The insights from this study are expected to provide researchers exploring electrochemistry at L-L interfaces with the means to provide a balanced analysis of their experimental data. As an example, by changing the aqueous electrolyte ion composition, we propose that shifts in the position of the potential of zero charge (PZC) at the ITIES, due to the nature of ions adsorbed, influences the kinetics of ion transfer.

2. Experimental methods

2.1 Materials

All chemicals were used as received without further purification. All aqueous solutions were prepared with ultra-pure water (Millipore Milli-Q, specific resistivity 18.2 M Ω -cm). Bis(triphenylphosphoranylidene) ammonium chloride (BACl, 97%) and lithium tetrakis(pentafluorophenyl)borate diethyletherate ([Li(OEt₂)]TB) were obtained from Sigma-Aldrich and Boulder Scientific Company, respectively. Bis(triphenylphosphoranylidene)ammonium tetrakis(pentafluorophenyl)borate (BATB) was prepared by metathesis of equimolar solutions of BACl and [Li(OEt₂)]TB in a methanol-water (2:1 v/v) mixture. The resulting precipitates were filtered, washed, recrystallised from acetone and finally washed 5 times with methanol-water (2:1 v/v) mixture. Lithium chloride (LiCl, $\geq 95\%$), aluminium sulfate (Al₂(SO₄)₃, 99.99%), tetraethylammonium chloride (TEACl, $\geq 98\%$), lithium sulfate (Li₂SO₄, $\geq 98.5\%$), methane sulfonic acid (MSA, $\geq 99\%$), and sulfuric acid (H₂SO₄, 95-98%) were obtained from Sigma-Aldrich. The organic solvent α,α,α -trifluorotoluene (TFT, 99+%) was obtained from Acros Organics.

2.2 Electrochemical measurements at the ITIES

Electrochemical experiments were carried out at the water | α,α,α -trifluorotoluene interface using a four-electrode configuration (the geometric area of the cell was 1.60 cm²). To supply the current flow, platinum counter electrodes were positioned in the organic and aqueous phases. The potential drop at the L-L interface was measured by means of *pseudo*-reference silver/silver chloride (Ag/AgCl) electrodes, which were connected to the aqueous and organic phases, respectively, through Luggin capillaries. In some experiments Ag/AgX

reference electrodes were used, where X is the anion with the highest concentration in the aqueous phase, to ensure reference potential stability. The Galvani potential difference was attained by assuming the formal ion transfer potential of TEA⁺ to be 0.149 V [29]. The general configuration of the cell is outlined in Scheme 1. From this point on, we are going to specify only the composition of the aqueous phase as all other elements of the 4-electrode electrochemical cell were kept constant.



Scheme 1. The general configuration of the four-electrode electrochemical cell used for cyclic voltammetry (CV) and AC voltammetry measurements. Only the aqueous electrolyte composition was varied between studies. The organic electrolyte solution was always α,α,α -trifluorotoluene (TFT) containing 5 mM bis(triphenylphosphoranylidene)ammonium tetrakis(pentafluorophenyl)borate (BATB).

Electrochemical impedance spectra were measured using an Autolab PGSTAT204 potentiostat with a frequency response analyzer module (FRA32M) and a four-electrode electrochemical cell. The AC amplitude was 10 mV and the frequency range was between 0.1 and 5×10^5 Hz. The potentiostat was connected to an uninterruptible power supply (APC by Schneider Electric) to ensure voltage stability and remove an inductive artefact at high frequencies. Differential capacitances at different applied voltages were measured using alternating current (AC) voltammetry, also known as potentiodynamic electrochemical impedance spectroscopy (EIS), at 10 Hz and assuming the cell behaves as a series R-C circuit. At this frequency, the contribution of faradic processes is significant only at the edge of the potential window.

3 Results and discussion

3.1 Interpreting EIS spectra at the ITIES across a broad range of frequencies (500 kHz to 0.1 Hz)

The high frequency behaviour observed in EIS spectra at a polarised ITIES has been attributed to stray capacitance and resistance associated with the parasitic coupling of the reference and counter electrodes, as well as to the resistance of the bulk solution [24,30]. Wiles *et al.* [15]

suggested that the high frequency behaviour comes from artefacts due to both the cell and reference arm resistances of the organic phase, and stray capacitances of the potentiostat and leads. While all of these hypotheses are reasonable, they remain unproven. Key issues are the assumptions that the organic and aqueous electrolytes behave as an ideal resistance in the frequency range between 1 MHz and 0.1 Hz (*i.e.*, following Ohm's "law") and that all capacitors have a fixed capacitance at all frequencies (*i.e.*, there is no dielectric relaxation at the frequencies). Ohm's "law" is a phenomenological equation (meaning empirical) that is not universal and that electrolyte solutions and interfaces are not ideal dielectrics. Therefore, a key question to be addressed is: can we distinguish which experimental conditions cause the EIS spectra to show true artefacts or, instead, solvent polarisation and a non-linear behaviour of the system?

Developing a comprehensive understanding of EIS spectra at the ITIES across a broad range of frequencies, from 500 kHz to 0.1 Hz, is challenging. In order to deconvolute the signal, EIS spectra were recorded for a 4-electrode electrochemical cell filled solely with an aqueous (red data in Fig. 1) or organic (blue data in Fig. 1) electrolyte solution, or with two immiscible electrolyte solutions forming the ITIES (black data in Fig. 1). The electrochemical cell used resembles a four-point probe setup to measure the electrical impedance of a material or electrolyte. This technique uses separate pairs of current-carrying and voltage-sensing electrodes to make more accurate measurements than those possible with two-terminal sensing. *As all EIS spectra presented in Fig. 1 were obtained using the same experimental setup, the impedance coming from cables, cell configuration and instrumentation were the same.* Fig. 1 and Table 1 show that (a) the aqueous and organic electrolytes behave as an ideal resistance only at frequencies lower than 50 kHz and 276 Hz, respectively; (b) the resistance at lower frequencies of the organic electrolyte is ~7 times higher than the one for the aqueous electrolyte; (c) the aqueous electrolyte presents an inductive behavior at frequencies around 50 kHz and (d) that both electrolytes behave as dielectric materials at high frequencies. Fig. 1 clearly shows that the organic electrolyte resistance (related to ionic conduction) is in parallel with capacitors of low (nF) capacitance (blue data), which can be seen at high frequencies.

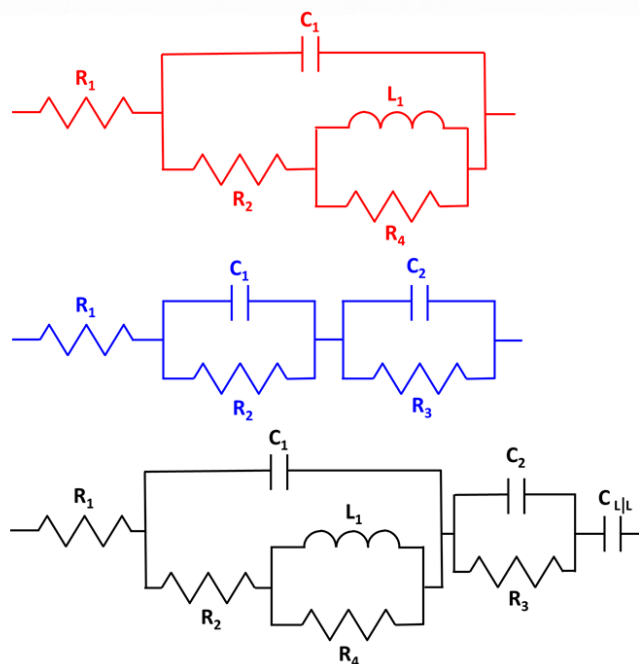
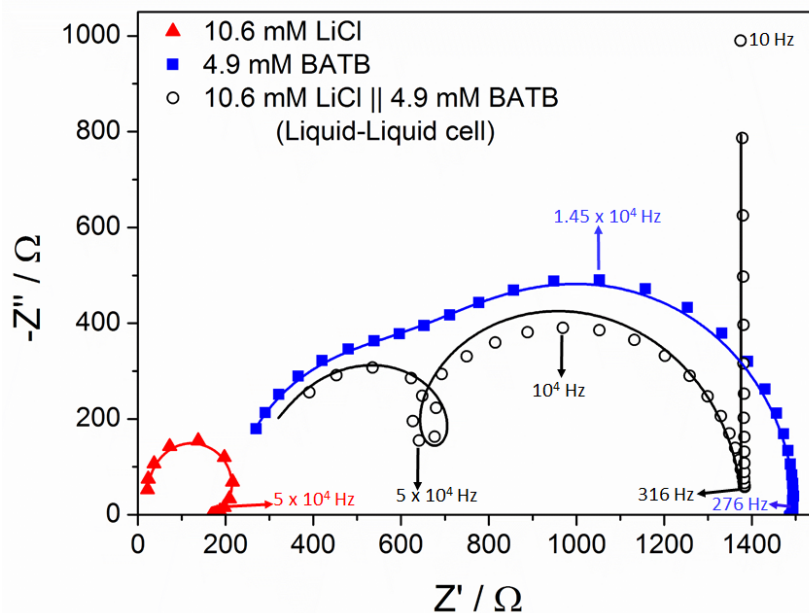


Fig. 1. Electrochemical impedance spectroscopy (EIS) spectrum of the 4-electrode L-L electrochemical cell glassware filled with (red triangles) an aqueous solution of 10.6 mM LiCl, (solid blue squares) 4.9 mM BATB in TFT, or (open black circles) two immiscible electrolyte solutions, 10.6 mM LiCl (aq) and 4.9 mM BATB in TFT, forming the ITIES. The solid lines show the simulated spectra using the shown electric circuits. The values of each element of the circuits are shown in Table 1. In this figure each colour belongs to the same electrochemical cell. The blue and red data were divided by 2 in order to normalise the data to the expected values where the ITIES is present.

Table 1. Electric elements used to fit the experimental data shown in Fig. 1.

Element	10.6 mM LiCl	4.9 mM BATB	10.6 mM LiCl / 4.9 mM BATB	Maximum error %
R ₁ (Ω)	37	430	254	9.6
R ₂ (Ω)	300	869	127	17
R ₃ (Ω)	--	1697	993	4
R ₄ (Ω)	1x10 ⁶ *	--	350	8
C ₁ (nF)	4.8	1.7	2.8	13
C ₂ (nF)	--	6.6	12.7	11
C _{L/L} (μF)	--	--	15.9	24
L ₁ (mH)	0.43*	--	1*	--

*These values were fixed to ensure convergence of the fitting.

The EIS spectrum of the ITIES shows two new features in comparison to the EIS spectrum of just the organic phase; first, a capacitor, seen at frequencies between 316 Hz and 10 Hz. This is created by the two back-to-back diffuse double layers that are present in series with the equivalent circuit associated with the organic phase. The second feature is observed at ~50 kHz, and is an inductive loop possibly due to the presence of the aqueous electrolyte that shows an inductive behavior at approximately the same frequencies. Also this loop may be due to ionic polarisation of the double layer, inductance from the cables, or another artefact from the high resistance of the organic reference electrode [31]. Fig. 1 demonstrates that the electrolytes in the 4-electrode L-L cell are not ideal resistances and their impedances are frequency dependent. The frequencies where the impedance is mainly real are ca. 300 to 500 Hz. Thus, the impedance values at those frequencies may be taken as the electrolyte resistance and used, for example, to implement the iR compensation. Usually the features of the EIS spectrum at frequencies higher than 1000 Hz have been assigned to artefacts [24]. Indeed, some artefacts can be seen at those frequencies and it is why the potentiostat must be connected to an uninterruptible power supply to ensure voltage stability and remove an inductive artefact at high frequencies, the electric connections must be as short as possible, and the L-L cell must be inside a Faraday cage. However, Fig. 1 suggests that the origin of the features at high frequency are dielectric relaxation processes in the bulk of the electrolytes and at the L-L interface, as explained in the next section. Therefore, elimination of

dielectric relaxation and/or all artefacts from the electrochemical cell to measure the electrolyte resistance related to the charge transport of ions is not necessary if the data are taken at frequencies lower than 500 Hz.

Usually a frequency between 2 and 10 Hz are used to measure the capacitance of the ITIES, but the impedance at frequencies lower than 10 Hz has a significant contribution from a Warburg element related to mass transport phenomena of ions at the interface. Thus, we recommend the use of frequencies between 10 and 80 Hz to measure the capacitance of the ITIES. The frequencies of 50 Hz or 60 Hz have to be avoided because of the presence of external noise coming from the external power supply.

3.2 The mechanism by which the potential drop at the L-L interface changes when the potential difference between the two counter electrodes is changed

It is important to state that the interfacial capacitance is affected by the dielectric properties of the solvents. When interfaces and electrolytes are polarised in AC fields, various polarisation mechanisms can be observed and their permittivity shows frequency dependence, namely dielectric relaxation or dielectric dispersion [32]. The permittivity depends on the frequency of the applied electric field as it has contributions from orientation, vibration and electronic polarisation in polar liquid. On the other hand, different polarisation mechanisms have been observed on the electrical double layer for different times after the application of the field [33]. To our knowledge, no research has been published concerning the dielectric properties of the organic electrolytes of BATB in TFT and the polarised ITIES. Many cases of dielectric low frequency relaxation (in the range of Hz and kHz) have been reported for polymer electrolytes, organic tissues and interfaces [34,35]. The origin of the low frequency relaxation is unknown, but it has been suggested that it comes from counter-ion polarisation at the electric double layers and/or ion pair polarisation.

From the data shown in Fig. 1, the 4-electrode L-L electrochemical cell resistance is mainly attributed to the resistance of the organic phase. Thus, *the iR drop happens primarily in the organic solvent, which is polarised under the applied potential.* As a result, the bulk potential of the aqueous phase is almost constant during potential cycling, whereas the potential of the bulk organic phase undergoes significant change. While the interface between a metallic electrode and an electrolyte solution is also polarisable, the polarisation mechanism at the ITIES is different. When the electrode-electrolyte interface is polarised, the potential in the bulk electrolyte solutions

remains almost constant, and the Fermi level of the solid electrode changes. However, the concept of a Fermi level is not applicable to electrolytes dissolved in a liquid (unless redox couples are present, as the potential in the bulk electrolyte is not constant if there is current flow).

Therefore, an obvious question is: how can the potential difference at the L-L interface be affected by the potential difference between the two counter electrodes? Liquids do not have a Fermi level. The only way to change their bulk potential is by changing the proportion of ions (breaking the charge balance) in each bulk phase, which is unlikely at ambient room conditions, or by changing the dipole moment per volume, which is likely [11]. While breaking the charge balance in each bulk phase is unlikely, electroneutrality may be broken at a small distance, *e.g.*, Johans *et al.* [36] showed using NMR that by addition of salts composed of a hydrophilic and a hydrophobic ion (potential determining salts) to a microemulsion, the salt primarily dissociated across the interface. In other words, the hydrophobic ion resided on the oil side of the surfactant monolayer and the hydrophilic ion on the water side, breaking electroneutrality in both microdomains [36].

Interestingly, *only those interfaces formed between polar solvents are suitable to study electrochemical reactions, such as ion transfer, upon external polarisation using a potentiostat.* This is why solvents such as TFT ($E_T^N = 0.241$), nitrobenzene ($E_T^N = 0.324$) and DCE ($E_T^N = 0.327$) are suitable for these kinds of experiments. E_T^N refers to the solvent polarity scale based on the normalised molar electronic transition energies of a probe molecule [37]. The lower limit of polarity required for an organic solvent to successfully form a polarised interface with water is still unclear, with toluene ($E_T^N = 0.099$) [38,39] and chloroform ($E_T^N = 0.259$) [40,41] used to create polarised micro-ITIES. On the other hand, excessively polar solvents cannot be polarised with water, as the solvation of ions is too similar (leading to tiny polarisable potential windows). Butyronitrile is on the limit ($E_T^N = 0.333$) in this regard, providing a small 200 mV polarisable potential window [42], with acetonitrile ($E_T^N = 0.460$) [43,44] and propylene carbonate ($E_T^N = 0.491$) [45] too similar to water.

The difference of potential, or electrical potential energy, between two bulk liquids is due to the difference of their individual dipolar momentum per volume [11]. This is why a polar organic solvent is a prerequisite to form a polarised interface with water. The potential difference across the interface can be changed using a potentiostat and the 4-electrode cell. If the molecules

that form the liquid possess a permanent ground state dipole moment, the molecules will tend to reorient in the applied field. In other words, *the ability of the dipoles or multipoles to change their orientations to minimise their free energies leads to interfacial and bulk polarisation* [46]. This is the mechanism by which a liquid can store electric potential energy (mainly at the interface, but also in the entire bulk organic phase where a significant iR drop takes place), and the potential between two polar liquids can be changed externally using a potentiostat or power supply. Polar molecules tend to align in an applied electric field due to the torque of the applied field in the frequency range of $10^6 - 10^{10}$ Hz [32,46].

In the literature, the dielectric properties (especially those that are non-linear and non-ideal) of the solvents, electrolytes and interfaces are usually ignored for data analysis [11,46]. A possible explanation is that inclusion of solvent polarisability in condensed-phase computational models is non-trivial due to the many-body character of polarisability effects and their non-linear behaviour [32,46]. On the other hand, the electric field along the direction perpendicular to the solvent junction is not easy to predict due to complexity associated with the presence of a gradient of permittivity, solvent polarity and adsorption of ions at the interface [11,32,46].

3.3 Capacitive and faradic currents at the ITIES

Upon formation, the ITIES is away from equilibrium and permeable to ions to some extent at open circuit potential and across the whole potential window. Therefore, the ITIES should be considered as a close approximation, but not a perfect realisation, of an ideally polarisable interface [11]. At solid electrodes, the polarisability of the solid-electrolyte interface is defined in terms of the exchange current density, i_0 . Hence, a broad potential window does not mean that only capacitive current is flowing, rather that the faradaic contribution is just low. The concept of i_0 can also be applied at the ITIES. For example, if the solvents are too close to each other in terms of their polarity, the electrolytes are mixed easily (for example water and propylene carbonate, $\epsilon = 66.1$ [45]), making i_0 higher and the potential window narrower.

Here, we address the origin of the currents seen across the whole potential window when a L-L interface is polarised. Fig. S1, Supporting Information (SI), shows the effect of the chosen potential range on the currents observed with staircase voltammetry across the potential window when an aqueous 10.6 mM LiCl electrolyte is used. Currents in the

middle of the potential window depend on the limits of the potential used for cycling; in other words, the currents increase when a wider potential range is scanned. This behavior is not expected when only capacitive currents are measured. Thus, it is clear that *the contribution of faradaic currents is significant across the full range of the polarisable potential window, i.e. i_0 is non-negligible.*

The contribution of capacitive currents can be observed at scan rates higher than $50 \text{ mV}\cdot\text{s}^{-1}$ (Fig. 2). The voltammograms shown in Fig. 2 at scan rates higher than $50 \text{ mV}\cdot\text{s}^{-1}$ are very symmetric and the potential of zero charge (PZC) can be clearly seen. Furthermore, at scan rates lower than $100 \text{ mV}\cdot\text{s}^{-1}$, the iR drop is insignificant (less than 4 mV). Therefore, it is possible to study capacitive currents and adsorption processes with CV at $100 \text{ mV}\cdot\text{s}^{-1}$ and using a potential window where the currents are not higher than about $2 \mu\text{A}\cdot\text{cm}^{-2}$. Meanwhile, at low scan rates, a shift of the voltammogram to negative currents is observed (Fig. 2, inset). The latter corroborates the presence of ionic currents across the whole potential window. Taking into account that the Cl^- ions have low hydration energy and small ionic radius, it is very likely that Cl^- transfer is the origin of this negative shift of the voltammogram.

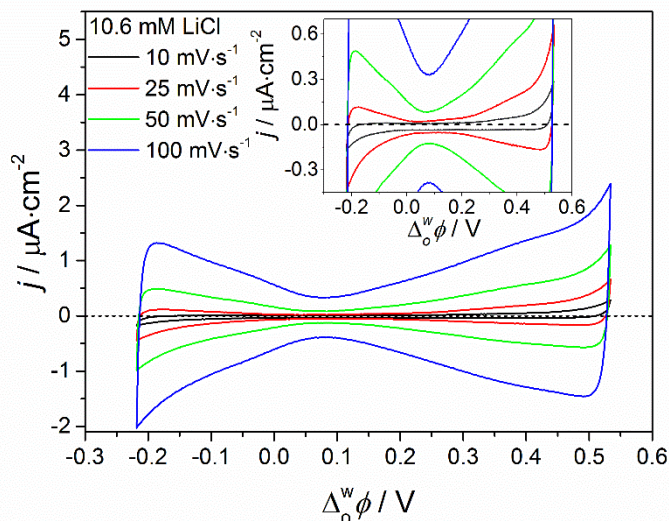


Fig. 2. Cyclic voltammetry (CV) at different potential scan rates ($10, 25, 50$ and $100 \text{ mV}\cdot\text{s}^{-1}$) when the aqueous electrolyte is 10.6 mM LiCl in Scheme 1. (inset) Zoom-in on CVs at potential scan rates of 10 and $25 \text{ mV}\cdot\text{s}^{-1}$. The dotted line represents zero current and clearly shows that at slow scan rates the voltammograms shift to negative currents.

Usually the potential dependence of the capacitance has been extracted from the impedance spectrum through fitting to a Randles circuit [21,22]. This means that across the whole potential range a Warburg element, related to faradaic currents controlled by diffusion, is needed. This fact confirms once more the observation of faradic currents across the whole potential window. Furthermore, Kontturi and co-workers [22] stated that “a problem with the measurement of the capacitance at the interface of immiscible electrolytes is the presence of residual currents due to ion transfer within the potential range of interest.” Upon extensively reviewing the literature, we have not found any other explicit references regarding the influence of residual ion transfer within the polarisable potential window, and none related to CV measurements.

When analysing voltammetry data obtained at the ITIES, it can be noted that the ions have affinity to only one solvent (either aqueous or organic) or the bulky ions of the organic phase may move to the aqueous phase [21]. For example, bulky ions of the organic phase may transfer to the aqueous phase, as BACl for example is moderately soluble in water. Indeed, the reference potential for the organic phase is realised by a secondary aqueous-organic interface, with the potential fixed at this interface by BA^+ as a shared common ion. As BA^+ is relatively soluble in water, 1 mM BACl is dissolved in the organic reference solution to minimise artefacts associated with the reference electrode potential by safeguarding a defined Nernst-Donnan potential difference between the organic reference solution and BATB in the bulk organic phase [47,48]. At lower concentrations, the potential shifts significantly over time due to the continuous partition of BA^+ from the organic phase to the organic reference solution.

3.4 Electrochemical monitoring of the electro-adsorption of small inorganic ions at the ITIES

The classical description of the electrical double layer at the ITIES employs the Gouy–Chapman model that assumes that the inner layer is a charged plane, where ionic adsorption takes place. It has been reported that ion–ion interactions, without specific adsorption, manifest as an asymmetry in the capacitance response without a corresponding shift of the capacitance minimum [26]. The adsorption of ionic species manifests itself as an increase of the differential capacitance

and the shifting of the minimum of the capacitance to positive values if only anions are adsorbed, or to negative values if only cations are adsorbed [27].

Fig. 3a shows the differential capacitance at different applied potentials for different aqueous electrolytes. We note five major observations from Fig. 3a. First, the cell with 5 mM H_2SO_4 has a lower capacitance at the PZC than the cell with 5 mM Li_2SO_4 . It seems that the ionic strength is lower for H_2SO_4 , which is not dissociated completely at the interface. Second, at potentials much lower than the PZC (< 0.15 V), the curve for H_2SO_4 approaches the curve for Li_2SO_4 . This may be due to the increase in concentration of sulfate anions (SO_4^{2-}) at, and expulsion of protons from, the interface at negative potentials. This loss of protons (increasing the pH locally at the interface) enhances H_2SO_4 dissociation at the interface. The third major observation from Fig. 3a is that the shoulders on both sides of the curve for Li_2SO_4 suggest the adsorption of Li^+ and SO_4^{2-} at the interface at positive and negative potentials *vs.* PZC, respectively. The same analysis is valid for the case of MSA, with protons and methanesulfonate anions (MS^-) adsorbed at the interface at positive and negative potentials *vs.* PZC, respectively. To our knowledge, the adsorption of ions as H^+ , MS^- , SO_4^{2-} has not been reported previously. Studying different organic electrolytes, Pereira *et al.* [25] showed experimental and theoretical evidence that ion pairing and specific ion adsorption can take place at the ITIES, results that agree with the data shown in Fig. 3. We note also that the adsorption of Li^+ can be observed more clearly with Li_2SO_4 than LiCl . Finally, the V-shaped function and magnitude of the capacitances for LiCl are similar to those reported for the interface between aqueous solutions of Li^+ , Na^+ , K^+ , Rb^+ and Cs^+ chlorides and electrolytes dissolved in 1,2-dichloroethane or nitrobenzene [22].

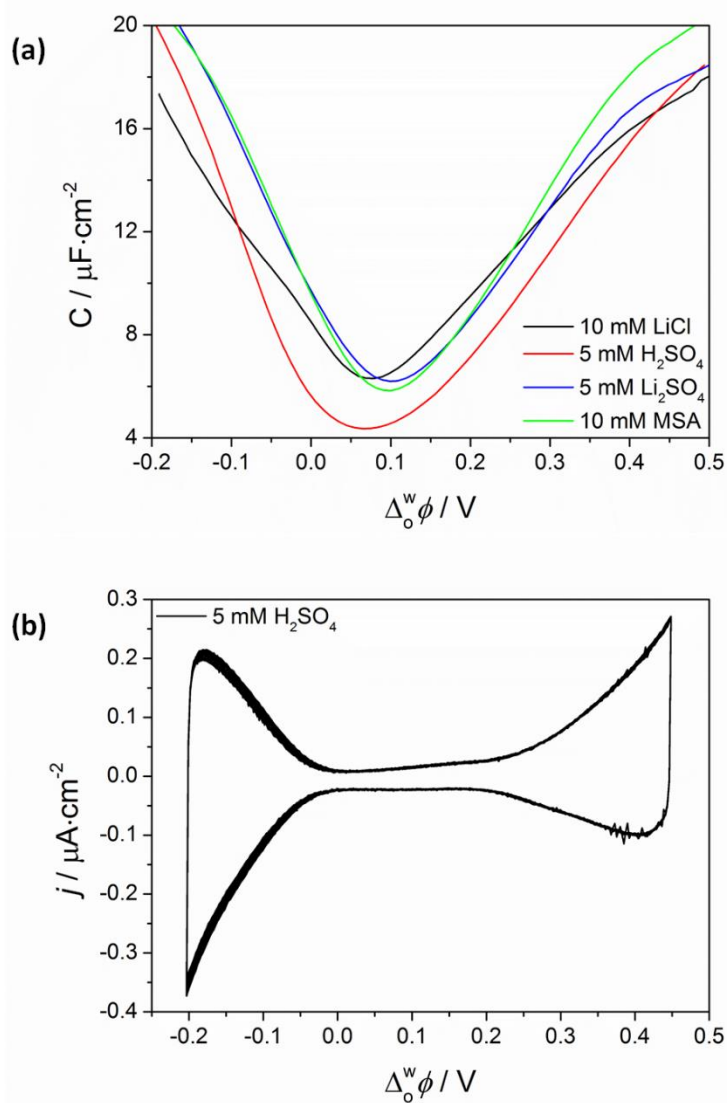


Fig. 3. (a) Differential capacitance curves for the aqueous electrolytes: (black line) 10 mM LiCl, (red line) 5 mM H_2SO_4 , (blue line) 5 mM Li_2SO_4 , and (green line) 10 mM MSA. (b) CV of the cell when the aqueous electrolyte is 5 mM H_2SO_4 in Scheme 1. Fifteen cycles at a scan rate $25 \text{ mV}\cdot\text{s}^{-1}$ are shown.

The voltammogram at $25 \text{ mV}\cdot\text{s}^{-1}$ when the aqueous electrolyte in Scheme 1 is 5 mM H_2SO_4 is shown in Fig. 3b. The shape of this voltammogram is different to the shape of the capacitive curve, which is expected because at low scan rates faradic currents are preferentially seen. However, in this regard, it is remarkable that at the centre of the

voltammogram no significant ionic currents are observed, indicating once again that the dissociation of H_2SO_4 at the interface and at the PZC is very low.

Differential capacitance curves are a powerful tool to study interfacial ion adsorption, and thereby obtain a deeper understanding of the structure of the electrical double layer at the L-L interface. Fig. 4a-b shows the differential capacitance curves for the aqueous electrolytes 5 mM H_2SO_4 and 10 mM LiCl in the absence and presence of $\text{Al}_2(\text{SO}_4)_3$ in the aqueous phase. The presence of Al^{3+} clearly increases the capacitances at potentials higher than the PZC, and the PZC shifts negatively, as expected for the adsorption of a cation such as Al^{3+} at the interface. Su *et al.* [27] simulated the effect of the adsorption of charged species on the differential capacitance vs. potential curve. *To our knowledge, this is the first experimental evidence that fits well to Su et al.'s digital simulations.* The curves in Fig. 4a-b are those expected when *the adsorption follows a Frumkin model and the Gibbs adsorption energy increases with the surface coverage.* The latter indicates a repulsive interaction between the adsorbed ions. Furthermore, in Fig. 4b, the adsorption of SO_4^{2-} clearly produces a slight shoulder at potentials lower than PZC.

The differential capacitance data in Fig. 4a-b also indicates that Al^{3+} adsorbs to a greater extent at the L-L interface when the aqueous phase is acidified. This observation is related to the distribution of the aluminium hydroxide complexes as a function of pH. Below pH 5 the most abundant species are $\text{Al}(\text{H}_2\text{O})_6^{3+}$ and $\text{AlOH}(\text{H}_2\text{O})_5^{2+}$, with $\text{Al}(\text{H}_2\text{O})_6^{3+}$ being the most abundant specie at acidic pH. Thus, a conclusion can be reached that $\text{Al}(\text{H}_2\text{O})_6^{3+}$ adsorbs more readily than other forms of Al^{3+} at the liquid-liquid interface. At higher pH the aluminium ion can be polymerised [49].

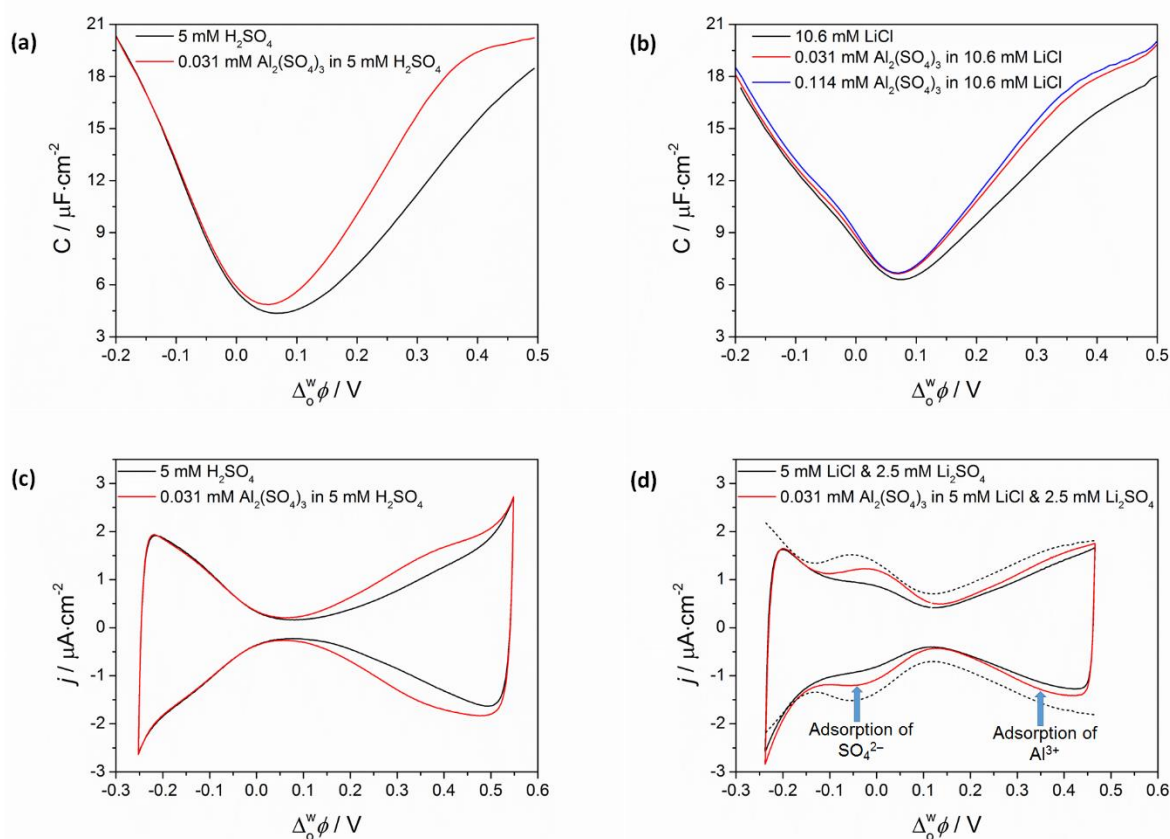


Fig. 4. Electrochemical monitoring of the electro-adsorption of Al^{3+} at the ITIES. (a-b) Differential capacitance vs. potential when the aqueous electrolyte in Scheme 1 was (a) 5 mM H_2SO_4 or (b) 10.6 mM LiCl in the absence or presence of $\text{Al}_2(\text{SO}_4)_3$ in the aqueous phase. The capacitances were measured using an AC frequency of 10 Hz. (c-d) CV when the aqueous electrolyte in Scheme 1 was (c) 5 mM H_2SO_4 or (d) 5 mM LiCl & 2.5 mM Li_2SO_4 in the absence or presence of $\text{Al}_2(\text{SO}_4)_3$ in the aqueous phase. The scan rate used was $100 \text{ mV}\cdot\text{s}^{-1}$. The dashed line is the expected voltammogram at $100 \text{ mV}\cdot\text{s}^{-1}$ calculated from the capacitances measured with AC voltammetry at 10 Hz. CV can also be used to study the adsorption of ions, with clear differences at positive potentials, indicating Al^{3+} adsorption, in the voltammograms obtained in the absence and presence of $\text{Al}_2(\text{SO}_4)_3$ in 5 mM H_2SO_4 (Fig. 4c). In order to observe SO_4^{2-} adsorption in the presence of $\text{Al}_2(\text{SO}_4)_3$ more clearly, the aqueous electrolyte was changed to 5 mM LiCl & 2.5 mM Li_2SO_4 . (Fig. 4d).

Indeed, SO_4^{2-} adsorption at the surface was observed (red CV in Fig. 4d), and the surface coverage increases with SO_4^{2-} concentration in the aqueous phase (not shown). At high concentrations of Cl^- , and at potentials lower than the PZC, the charge balance at the interface is controlled by Cl^- ions. Under these conditions, SO_4^{2-} adsorption is less probable. In other words, all ions can be competitively adsorbed at the ITIES but with very

different adsorption constants. This highlights the complexity of ion adsorption at the L-L interface, or in general for any system, in which the adsorption of one specific ion cannot be studied independently of other ions. In other words, it is very difficult to reliably predict the outcome of changing the concentration of only one ion, on the interactions of all ions present in the system.

Interestingly, the capacitances measured by AC voltammetry are very reproducible despite the fact that significant faradic currents are present all the time within the potential window, as discussed *vide supra*. For example, in Fig. 4a-b at potentials lower than the PZC, where no change is expected, the data deviation is very low. On the other hand, the capacitances measured by CV (Fig. S1, SI, and Fig. 2) depend on the limits of potential cycling and on the scan rate. Figure 4d clearly shows the difference between the capacitances measured by AC voltammetry and CV.

The larger solvation energy of Li^+ and its low electrical charge inhibit its adsorption and ability to approach the organic counter-ion, $[\text{B}(\text{C}_6\text{F}_5)_4]^-$ (typically denoted as TB^- in articles related to electrochemistry at the ITIES). Conversely, Al^{3+} adsorbs more strongly as it has a higher charge and can form an ion pair at the interface separated by the solvation shell of each ion. In other words, Al^{3+} can have a longer range electrostatic interaction than Li^+ . The same explanation is valid for the adsorption of SO_4^{2-} and unlikely adsorption of Cl^- . Salts of $[\text{B}(\text{C}_6\text{F}_5)_4]^-$ are used as supporting electrolytes in solvents with low permittivity because this anion is very effective at solubilising positively charged species due its low tendency to form ion pairs [50]. However, Fig. 4a-b shows that *at high polarisations the capacitance is significantly affected by interactions between oppositely charged species from different phases at the inner layer, i.e., between Al^{3+} and $[\text{B}(\text{C}_6\text{F}_5)_4]^-$.*

The dashed line in Fig. 4d shows the expected voltammogram calculated from the capacitances measured with AC voltammetry at 10 Hz for an aqueous electrolyte of 0.031 mM $\text{Al}_2(\text{SO}_4)_3$ in 5 mM LiCl & 2.5 mM Li_2SO_4 . The CV and AC voltammetry have the same qualitative features but the PZC differs and the capacitances measured by AC voltammetry are higher. The latter discrepancy has three probable sources: (i) during CV cycling there is not enough time to charge the interfacial capacitor, (ii) digital potentiostats filter some capacitive currents (because they apply step potentials and measure the current

at the end of each step), and (iii) the capillary waves generated by the AC voltage can increase the capacitance of the interface. Analysing the pros and cons of the capacitances measured by AC voltammetry, it can be concluded that those measurements do indeed describe interfacial processes at the ITIES and are more suitable for this kind of study than CV.

Differential capacitance measurements with an aqueous electrolyte solution containing methanesulfonic acid (MSA) are shown in Fig. 5 and Fig. 3a. From the shoulders on both sides of the PZC, it may be concluded that protons and MS^- anions can be adsorbed at the interface. Beyond the arrows at the edges of the potential window in Fig. 5, massive ionic currents are observed and the capacitances cannot be measured with high accuracy. Fig. 4a shows that in the positive potential range the capacitance increases in the order $H^+ > Li^+$, which is in agreement with their Gibbs energies of transfer [51].

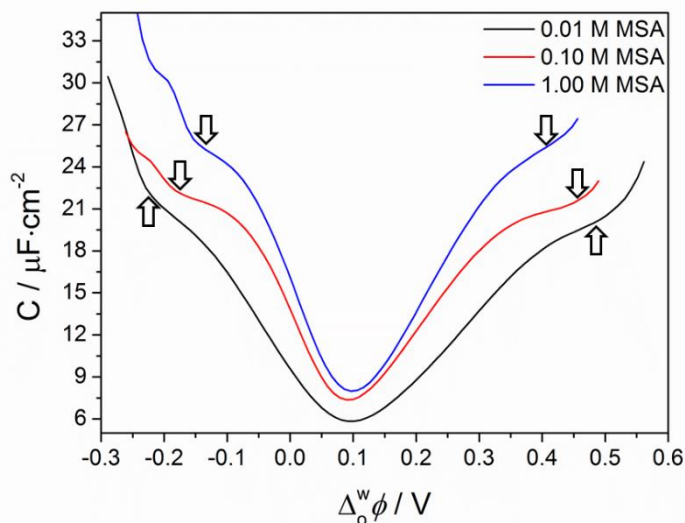


Fig. 5. Differential capacitance curves when the aqueous electrolyte in Scheme 1 was 0.01, 0.1 or 1 M methanesulfonic acid (MSA). At potentials beyond the arrows at the edges of the potential window, the signal was affected by extensive ion transfer and therefore is not completely related to the capacitance of the interface

At both positive and negative potentials far from the PZC and with more concentrated electrolytes (*e.g.*, 1 M MSA), the differential capacitance approaches a plateau (Fig. 5). This is because the ions in solution are tightly compressed at the L-L interface as

the electric field increases, and a Helmholtz capacitor is formed with the counter ions in different phases. At a very high concentration of electrolyte in the aqueous phase and at potentials close to the PZC, the composite capacitance is governed by the smaller of its constituent components, which is the capacitance of the electrical diffuse layer in the organic phase. This is why the capacitances at the PZC for the solutions of 0.1 and 1 M MSA are very similar, and the V-shaped function can still be observed at such high electrolyte concentrations. Unfortunately, due to solubility limitations, the electrolyte concentration of the organic phase cannot be changed too much in order to study this component of the total capacitance of the interface.

It can be concluded that *the Gouy-Chapman-Stern model gives predictions that account for the gross features of Fig. 5, but there are still some discrepancies*. For example, the Helmholtz capacitance is not independent of potential or electrolyte concentration. The origin of the latter can be due to changes of the dielectric properties, the structure of water and/or changes of the solvent polarity at the L-L interface. Previously, Schlossmann and co-workers reached a similar conclusion that predictions of the Gouy-Chapman theory vary substantially from their X-ray reflectivity measurements of the ITIES [28,52,53].

3.5 The effect of the structure of the electrical double layer and the adsorption of ions on the kinetics of ion transfer

To probe this phenomenon, the ion transfer of tetraethylammonium (TEA^+) cations was studied in two different aqueous electrolyte solutions: one where the PZC is very close to the TEA^+ formal ion transfer potential of 0.149 V (*i.e.*, 5 mM LiCl & 2.5 mM H_2SO_4) and another where these two values are different (*i.e.*, 10.6 mM LiCl), see Fig. S2, SI. The voltammogram for the ion transfer of TEA^+ when the aqueous electrolyte was 10.6 mM LiCl is shown in Fig. S2b, SI. The peak current heights decrease upon potential cycling and there is a significant contribution of background ionic currents; the shapes of the current on both sides of the voltammogram are not as expected for a diffusion-controlled process. When the electrolyte 5 mM LiCl & 2.5 mM H_2SO_4 was used (Fig. S2c, SI), the peak current heights do not decrease to the same extent upon potential cycling, *i.e.*, the signal is more stable as expected for a diffusion-controlled process.

The voltammograms with TEA^+ in Fig. S2, SI, indicate that the mass transport from the aqueous to organic phase is enhanced and cannot be explained solely by diffusion. We propose

that both diffusion and migration have to be taken into account in order to explain the rapid decrease of the peak current heights upon CV cycling. This suggests that *mass transport by migration is not negligible when the mass transfer takes place away from the PZC*. The low concentration of electrolyte used in the aqueous phase is not enough to compress the electrical double layer on the water side of the interface. Under these conditions, the thickness of the electrical layer is not negligible in comparison with the thickness of the Nernst diffusion layer, and thus migration is not negligible in comparison to diffusion. When the TEA⁺ ion transfer process is studied using a high concentration of aqueous electrolytes, the voltammograms are more stable in time, as expected (data not shown).

4 Conclusions

Herein, we demonstrate that during electrochemical experiments it is important to take into account that the ITIES is not at thermodynamic equilibrium, the electrolyte solution is not an ideal resistor (especially at high electric field frequencies), and the interface and electrolyte solutions can show non-linear dielectric properties. Deconvolution of electrochemical impedance spectra at the ITIES show that the *iR* drop happens primarily in the organic solvent, which is polarised under the applied potential. We demonstrate that as electrochemistry at the ITIES proceeds away from equilibrium, the contribution of faradaic currents is significant across the whole polarisable potential window. The use of AC voltammetry, over cyclic voltammetry measurements, to calculate the differential capacitance is recommended as it is a direct measurement and does not come from numerical analysis. The Gouy-Chapman-Stern model gives predictions that account for the gross features of the differential capacitance curves at the ITIES, but there are still some discrepancies, such as the Helmholtz capacitance not being independent of potential or electrolyte concentration. We demonstrate that small inorganic anions, such as sulfate anions and aluminium cations, can be adsorbed at the ITIES, and methanesulfonic acid is strongly adsorbed. This is the first experimental evidence that fits well to Su *et al.*'s digital simulations of the adsorption of ionic species at the ITIES [27]. A particularly interesting finding is that the capacitance of the ITIES at the PZC in the presence H₂SO₄ is much lower than for Li₂SO₄ at the same analytical concentration. This means that the ionic strength is much lower for the case of H₂SO₄ at the ITIES. The structure of the electrical double layer and adsorption of ions affects the kinetics of ion transfer. When the

aqueous electrolyte composition was modified such that the formal ion transfer potential of tetraethylammonium cations was away from the potential-of-zero charge (PZC), we propose that mass transport by migration was non-negligible.

Conflicts of interest

There are no conflicts of interest to declare.

Acknowledgements

M.D.S. acknowledges Science Foundation Ireland (SFI) under Grant no. 13/SIRG/2137 and the European Research Council through a Starting Grant (Agreement no. 716792). M.F.S.-H. acknowledges the “Universidad Nacional de Colombia” for allowing his sabbatical leave.

References

- [1] P. Peljo, H.H. Girault, Liquid/Liquid Interfaces, Electrochemistry at, in: *Encycl. Anal. Chem.*, John Wiley & Sons, Ltd, Chichester, UK, 2012.
doi:10.1002/9780470027318.a5306.pub2.
- [2] Z. Samec, Dynamic electrochemistry at the interface between two immiscible electrolytes, *Electrochim. Acta.* 84 (2012) 21–28. doi:10.1016/j.electacta.2012.03.118.
- [3] G. Herzog, Recent developments in electrochemistry at the interface between two immiscible electrolyte solutions for ion sensing, *Analyst.* 140 (2015) 3888–3896.
doi:10.1039/c5an00601e.
- [4] M.D. Scanlon, E. Smirnov, T.J. Stockmann, P. Peljo, Gold nanofilms at liquid-liquid interfaces: An emerging platform for redox electrocatalysis, nanoplasmonic sensors, and electrovariable optics, *Chem. Rev.* 118 (2018) 3722–3751.
doi:10.1021/acs.chemrev.7b00595.
- [5] P. Peljo, M.D. Scanlon, A.J. Olaya, L. Rivier, E. Smirnov, H.H. Girault, Redox

- electrocatalysis of floating nanoparticles: Determining electrocatalytic properties without the influence of solid supports, *J. Phys. Chem. Lett.* 8 (2017) 3564–3575. doi:10.1021/acs.jpcclett.7b00685.
- [6] L. Rivier, T.J. Stockmann, M.A. Méndez, M.D. Scanlon, P. Peljo, M. Opallo, H.H. Girault, Decamethylruthenocene hydride and hydrogen formation at liquid|liquid interfaces, *J. Phys. Chem. C.* 119 (2015) 25761–25769. doi:10.1021/acs.jpcc.5b08148.
- [7] S. Rastgar, G. Wittstock, Characterization of Photoactivity of Nanostructured BiVO₄ at polarized liquid–liquid interfaces by scanning electrochemical microscopy, *J. Phys. Chem. C.* 121 (2017) 25941–25948. doi:10.1021/acs.jpcc.7b09550.
- [8] J.B. Edel, A.A. Kornyshev, A.R. Kucernak, M. Urbakh, Fundamentals and applications of self-assembled plasmonic nanoparticles at interfaces, *Chem. Soc. Rev.* 45 (2016) 1581–1596. doi:10.1039/c5cs00576k.
- [9] S.G. Booth, R.A.W. Dryfe, Assembly of nanoscale objects at the liquid/liquid interface, *J. Phys. Chem. C.* 119 (2015) 23295–23309. doi:10.1021/acs.jpcc.5b07733.
- [10] L. Poltorak, A. Gamero-Quijano, G. Herzog, A. Walcarius, Decorating soft electrified interfaces: From molecular assemblies to nano-objects, *Appl. Mater. Today.* 9 (2017) 533–550. doi:10.1016/j.apmt.2017.10.001.
- [11] A.G. Volkov, ed., *Liquid Interfaces in Chemical, Biological, and Pharmaceutical Applications*. Surfactant Science Series. Volume 95, Marcel Dekker, Inc., New York and Basel, 2001.
- [12] F. Reymond, D. Fermín, H.J. Lee, H.H. Girault, Electrochemistry at liquid/liquid interfaces: methodology and potential applications, *Electrochim. Acta.* 45 (2000) 2647–2662. doi:10.1016/S0013-4686(00)00343-1.
- [13] I. Benjamin, Theoretical study of the water/1,2-dichloroethane interface: Structure, dynamics, and conformational equilibria at the liquid–liquid interface, *J. Chem. Phys.* 97 (1992) 1432–1445. doi:10.1063/1.463219.
- [14] J. Strutwolf, A.L. Barker, M. Gonsalves, D.J. Caruana, P.R. Unwin, D.E. Williams, J.R.P. Webster, Probing liquid|liquid interfaces using neutron reflection measurements and scanning electrochemical microscopy, *J. Electroanal. Chem.* 483 (2000) 163–173.

- doi:10.1016/S0022-0728(00)00027-9.
- [15] M.C. Wiles, D.J. Schiffrin, T.J. VanderNoot, A.F. Silva, Experimental artifacts associated with impedance measurements at liquid—liquid interfaces, *J. Electroanal. Chem. Interfacial Electrochem.* 278 (1990) 151–159. doi:10.1016/0022-0728(90)85130-W.
- [16] V. Mareček, Electrochemical monitoring of the co-extraction of water with hydrated ions into an organic solvent, *Electrochem. Commun.* 88 (2018) 57–60. doi:10.1016/j.elecom.2018.01.017.
- [17] K. Holub, Z. Samec, V. Mareček, Role of water in the mechanism of the salt extraction to the organic solvent, *Electrochim. Acta.* 306 (2019) 541–548. doi:10.1016/j.electacta.2019.03.096.
- [18] C.M. Pereira, A. Martins, M. Rocha, C.J. Silva, F. Silva, Differential capacitance of liquid/liquid interfaces: effect of electrolytes present in each phase, *J. Chem. Soc. Faraday Trans.* 90 (1994) 143–148. doi:10.1039/ft9949000143.
- [19] Z. Samec, J. Langmaier, A. Trojánek, Polarization phenomena at the water|*o*-nitrophenyl octyl ether interface Part II. Role of the solvent viscosity in the kinetics of the tetraethylammonium ion transfer, *J. Electroanal. Chem.* 426 (1997) 37–45. doi:10.1016/S0022-0728(96)05029-2.
- [20] D. Momotenko, C.M. Pereira, H.H. Girault, Differential capacitance of liquid/liquid interfaces of finite thicknesses: a finite element study, *Phys. Chem. Chem. Phys.* 14 (2012) 11268–11272. doi:10.1039/c2cp41437f.
- [21] L.I. Daikhin, M. Urbakh, Double layer capacitance and a microscopic structure of electrified liquid-liquid interfaces, *J. Electroanal. Chem.* 560 (2003) 59–67. doi:10.1016/j.jelechem.2003.06.009.
- [22] C. Yufei, V.J. Cunnane, D.J. Schiffrin, L. Mutomäki, K. Kontturi, Interfacial capacitance and ionic association at electrified liquid/liquid interfaces, *J. Chem. Soc., Faraday Trans.* 87 (1991) 107–114. doi:10.1039/FT9918700107.
- [23] Z. Samec, A. Trojánek, J. Langmaier, Origin of the effect of ion nature on the differential capacity of an interface between two immiscible electrolyte solutions, *J. Electroanal. Chem.* 444 (1998) 1–5. doi:10.1016/S0022-0728(97)00590-1.

- [24] Z. Samec, J. Langmaier, A. Trojánek, Evaluation of parasitic elements contributing to experimental cell impedance: impedance measurements at interfaces between two immiscible electrolyte solutions, *J. Chem. Soc., Faraday Trans.* 92 (1996) 3843–3849. doi:10.1039/FT9969203843.
- [25] C.M. Pereira, F. Silva, M.J. Sousa, K. Kontturi, L. Murtoimäki, Capacitance and ionic association at the electrified oil|water interface: the effect of the oil phase composition, *J. Electroanal. Chem.* 509 (2001) 148–154. doi:10.1016/S0022-0728(01)00528-9.
- [26] C.W. Monroe, M. Urbakh, A.A. Kornyshev, Understanding the anatomy of capacitance at interfaces between two immiscible electrolytic solutions, *J. Electroanal. Chem.* 582 (2005) 28–40. doi:10.1016/j.jelechem.2005.04.031.
- [27] B. Su, N. Eugster, H.H. Girault, Simulations of the adsorption of ionic species at polarisable liquid|liquid interfaces, *J. Electroanal. Chem.* 577 (2005) 187–196. doi:10.1016/j.jelechem.2004.11.030.
- [28] G. Luo, S. Malkova, J. Yoon, D.G. Schultz, B. Lin, M. Meron, I. Benjamin, P. Vanýsek, M.L. Schlossman, Ion distributions near a liquid-liquid interface, *Science*. 311 (2006) 216–218. doi:10.1126/science.1120392.
- [29] E. Smirnov, P. Peljo, M.D. Scanlon, H.H. Girault, Gold nanofilm redox catalysis for oxygen reduction at soft interfaces, *Electrochim. Acta.* 197 (2016) 362–373. doi:10.1016/j.electacta.2015.10.104.
- [30] B. Hou, P. Vanýsek, W. Bu, M.L. Schlossman, G. Luo, Ion distributions at electrified water-organic interfaces: PB-PMF calculations and impedance spectroscopy measurements, *J. Electrochem. Soc.* 162 (2015) H890–H897. doi:10.1149/2.0621512jes.
- [31] D. Lloyd, T. Vainikka, M. Ronkainen, K. Kontturi, Characterisation and application of the Fe(II)/Fe(III) redox reaction in an ionic liquid analogue, *Electrochim. Acta.* 109 (2013) 843–851. doi:10.1016/j.electacta.2013.08.013.
- [32] K. Asami, Characterization of heterogeneous systems by dielectric spectroscopy, *Prog. Polym. Sci.* 27 (2002) 1617–1659. doi:10.1016/S0079-6700(02)00015-1.
- [33] V.N. Shilov, A.V. Delgado, F. González-Caballero, J. Horno, J.J. López-García, C. Grosse, Polarization of the electrical double layer. Time evolution after application of an

- electric field, *J. Colloid Interface Sci.* 232 (2000) 141–148. doi:10.1006/jcis.2000.7152.
- [34] Q. Lu, K. Zhao, Dielectric spectroscopy of a nanofiltration membranes–electrolyte solution system: I. Low-frequency dielectric relaxation from the counterion polarization in pores and model development, *J. Phys. Chem. B.* 114 (2010) 16783–16791. doi:10.1021/jp110160z.
- [35] D. Miklavčič, N. Pavšelj, F.X. Hart, Electric Properties of Tissues, in: *Wiley Encycl. Biomed. Eng.*, John Wiley & Sons, Inc., Hoboken, NJ, USA, 2006: pp. 1–12. doi:10.1002/9780471740360.ebs0403.
- [36] C. Johans, M.A. Behrens, K.E. Bergquist, U. Olsson, J.A. Manzanares, Potential determining salts in microemulsions: Interfacial distribution and effect on the phase behavior, *Langmuir.* 29 (2013) 15738–15746. doi:10.1021/la404263v.
- [37] C. Reichardt, Solvatochromic dyes as solvent polarity indicators, *Chem. Rev.* 94 (1994) 2319–2358. doi:10.1021/cr00032a005.
- [38] M. Kasuno, Y. Matsuyama, M. Iijima, Voltammetry of ion transfer at a water-toluene micro-interface, *ChemElectroChem.* 3 (2016) 694–697. doi:10.1002/celec.201500568.
- [39] C. Liu, P. Peljo, X. Huang, W. Cheng, L. Wang, H. Deng, Single organic droplet collision voltammogram via electron transfer coupled ion transfer, *Anal. Chem.* 89 (2017) 9284–9291. doi:10.1021/acs.analchem.7b02072.
- [40] H. Ohde, A. Uehara, Y. Yoshida, K. Maeda, S. Kihara, Some factors in the voltammetric measurement of ion transfer at the micro aqueous|organic solution interface, *J. Electroanal. Chem.* 496 (2001) 110–117. doi:10.1016/S0022-0728(00)00367-3.
- [41] T.J. Stockmann, J.-M. Noël, A. Abou-Hassan, C. Combellas, F. Kanoufi, Facilitated Lewis acid transfer by phospholipids at a (water|CHCl₃) liquid|liquid interface toward biomimetic and energy applications, *J. Phys. Chem. C.* 120 (2016) 11977–11983. doi:10.1021/acs.jpcc.6b02354.
- [42] J.S. Riva, V.C. Bassetto, H.H. Girault, A.J. Olaya, Standard ion transfer potential at the water|butyronitrile interface, *J. Electroanal. Chem.* 835 (2019) 192–196. doi:10.1016/j.jelechem.2019.01.041.

- [43] J.C. Hidalgo-Acosta, M.A. Méndez, M.D. Scanlon, H. Vrabel, V. Amstutz, W. Adamiak, M. Opallo, H.H. Girault, Catalysis of water oxidation in acetonitrile by iridium oxide nanoparticles, *Chem. Sci.* 6 (2015) 1761–1769. doi:10.1039/c4sc02196g.
- [44] J.D. Watkins, F. Amemiya, M. Atobe, P.C. Bulman-Page, F. Marken, Liquid | liquid biphasic electrochemistry in ultra-turrax dispersed acetonitrile | aqueous electrolyte systems, *Electrochim. Acta.* 55 (2010) 8808–8814. doi:10.1016/j.electacta.2010.07.104.
- [45] E. Smirnov, P. Peljo, H.H. Girault, Self-assembly and redox induced phase transfer of gold nanoparticles at a water-propylene carbonate interface, *Chem. Commun.* 53 (2017) 4108–4111. doi:10.1039/c6cc09638g.
- [46] D. V. Matyushov, Electrostatics of liquid interfaces, *J. Chem. Phys.* 140 (2014) 224506. doi:10.1063/1.4882284.
- [47] Z. Samec, V. Mareček, J. Koryta, M.W. Khalil, Investigation of ion transfer across the interface between two immiscible electrolyte solutions by cyclic voltammetry, *J. Electroanal. Chem. Interfacial Electrochem.* 83 (1977) 393–397. doi:10.1016/S0022-0728(77)80186-1.
- [48] Z. Samec, V. Mareček, J. Weber, Charge transfer between two immiscible electrolyte solutions. Part II. The investigation of Cs⁺ ion transfer across the nitrobenzene/water interface by cyclic voltammetry with IR drop compensation, *J. Electroanal. Chem. Interfacial Electrochem.* 100 (1979) 841–852. doi:10.1016/S0022-0728(79)80203-X.
- [49] J.D. Hem, C.E. Roberson, Form and stability of aluminum hydroxide complexes in dilute solution, 1967. doi:10.3133/wsp1827A.
- [50] R.J. LeSuer, W.E. Geiger, Improved electrochemistry in low-polarity media using tetrakis(pentafluorophenyl)borate salts as supporting electrolytes, *Angew. Chemie Int. Ed.* 39 (2000) 248–250. doi:10.1002/(SICI)1521-3773(20000103)39:1<248::AID-ANIE248>3.0.CO;2-3.
- [51] F. Scholz, R. Gulaboski, Determining the Gibbs energy of ion transfer across water-organic liquid interfaces with three-phase electrodes, *ChemPhysChem.* 6 (2005) 16–28. doi:10.1002/cphc.200400248.
- [52] G. Luo, S. Malkova, S.V. Pingali, D.G. Schultz, B. Lin, M. Meron, T.J. Graber, J.

Gebhardt, P. Vanysek, M.L. Schlossman, X-ray studies of the interface between two polar liquids: Neat and with electrolytes, *Faraday Discuss.* 129 (2005) 23–34.

doi:10.1039/b405555a.

- [53] N. Laanait, M. Mihaylov, B. Hou, H. Yu, P. Vanysek, M. Meron, B. Lin, I. Benjamin, M.L. Schlossman, Tuning ion correlations at an electrified soft interface, *Proc. Natl. Acad. Sci.* 109 (2012) 20326–20331. doi:10.1073/pnas.1214204109.